

Cost-effective Variational Active Entity Resolution

Alex Bogatu^{†‡}, Norman W. Paton[†], Mark Douthwaite[‡], Stuart Davie[‡], André Freitas[†]

[†]University of Manchester, UK [‡]Peak AI Ltd.

alex.bogatu@manchester.ac.uk

Abstract—Accurately identifying different representations of the same real-world entity is an integral part of data cleaning and many methods have been proposed to accomplish it. The challenges of this entity resolution task that demand so much research attention are often rooted in the task-specificity and user-dependence of the process. Adopting deep learning techniques has the potential to lessen these challenges. In this paper, we set out to devise an entity resolution method that builds on the robustness conferred by deep autoencoders to reduce human-involvement costs. Specifically, we reduce the cost of training deep entity resolution models by performing unsupervised representation learning. This unveils a transferability property of the resulting model that can further reduce the cost of applying the approach to new datasets by means of transfer learning. Finally, we reduce the cost of labeling training data through an active learning approach that builds on the properties conferred by the use of deep autoencoders. Empirical evaluation confirms the accomplishment of our cost-reduction desideratum, while achieving comparable effectiveness with state-of-the-art alternatives.

I. INTRODUCTION

Entity Resolution (ER), or the process of identifying different representations of the same real-world entity, has been the subject of more than 70 years of research. Yet, practitioners often opt for *ad hoc* ER approaches mainly due to deficiencies in adapting existing solutions to new and specialized datasets. In practice, adapting an ER solution to a new use-case often translates to (1) mapping the types of features that govern the comparison of two entities and are expected by the adopted solution to the case at hand, i.e., *feature engineering*; (2) identifying local examples of duplicates and non-duplicates, i.e., *data labeling*; and (3) learning a task-specific similarity function that discriminates between duplicates and non-duplicates, i.e., *similarity learning*. Despite the sheer number of ER methods available [1], few solutions manage to reduce the costs incurred by the above triple, costs often paid in active user involvement and long configuration and training times.

With respect to (1) and (3) above, recent proposals (e.g., [2], [3]) resort to deep learning techniques [4] to adapt general-purpose features (e.g., word-embeddings [5], [6]) to new ER use-cases and learn a task-specific similarity function *concomitantly*. However, this is done at the expense of (2), since the resulting solutions tend to have a voracious appetite for labeled data (e.g., up to thousands of labeled instances [3]), and at the expense of training time, since such approaches can take up to hours to generalize. With respect to (2) above, recent deep ER-focused active learning proposals (e.g., [7]) aim to generate labeled data for merely adapting an existing and already trained entity matching model to the case at hand.

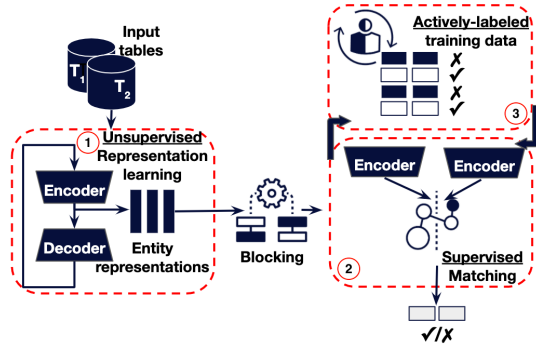


Fig. 1: Decoupled, cost-effective ER process

Therefore, there is limited support for manually labeling the volumes of training data often required by deep learning ER.

In this paper, we aim to reduce the costs associated with performing deep learning-based ER in practice by pioneering the use of Variational Auto-Encoders (VAEs) [8] for automatically generating entity representations. This allows us to *decouple feature engineering from similarity learning*, perform the former without user supervision (step 1 in Figure 1), and only rely on supervised learning for the latter (step 2 in Figure 1). Additionally, we support the data labeling effort for the supervised step through a proposed active learning technique (step 3 in Figure 1), facilitated by the above-mentioned decoupling. Therefore, our central contribution in this paper is an ER method that learns similarity functions over an unsupervised feature space and we show its cost-effectiveness potential through:

- An *unsupervised* and *transferable* representation learning method for producing similarity-preserving feature vectors for tuples (i.e., entities). Unsupervised because it builds on deep generative models (e.g., VAE) to automatically generate the feature vectors. Transferable because the resulting model is reusable without re-training across different ER scenarios and data domains.
- An *adaptable* matching method for learning task-specific similarity functions. Adaptable because it builds on Siamese neural networks [9] to fine-tune previously learned tuple representations to better reflect the notion of similarity derived from given training data.
- An *active-learning* scheme for assisting the user in labeling supervised matching training instances. Our contribution here is the exploitation of the generative property of VAEs to identify tuple pairs that are informative, diverse, and

balanced with respect to the match/non-match classes.

- An empirical evaluation of the above on a multitude of domains, demonstrating their collective potential for ER cost reduction in terms of (i) feature engineering and similarity learning; (ii) training times; and (iii) data labeling efforts.

II. BACKGROUND AND RELATED WORK

Typically, ER methods for structured data (e.g., [1], [10], [11]) include at least a *blocking* and a *matching* step [12]. The latter, which is the focus of this paper, involves detailed comparison of candidates efficiently identified by the former, often resorting to rule-based reasoning (e.g., [13], [14]), classification (e.g., [2], [15], [16]), crowdsourcing (e.g., [17], [18]), or generative modeling (e.g., [19]) to do so.

In this paper, we focus on *classification-based* matching. In practice, it often relies on string similarities between attribute values of tuples (e.g., [15], [16]). Alternatively, NLP-specific feature engineering methods (e.g., [4], [6]) are employed to extract meaningful numerical features from attribute values. These are then passed to deep learning [4] classifiers that learn a similarity function consistent with given duplicate/non-duplicate training examples [2], [3], [20]. Our proposal in this paper, **Variational Active Entity Resolution (VAER)**, is a *deep learning* ER solution that focuses on reducing the human-involvement cost of performing ER in practice. Specifically, deep learning ER proposals, such as *DeepER* [2], *DeepMatcher* [3], or *Seq2SeqMatcher* [20], aim to perform feature engineering and match training simultaneously, using the same training instances. This leads to complex models with many parameters to optimize that require thousands of labeled instances and potentially hours of training [3]. Conversely, VAER decouples the feature engineering and matching tasks, conducting the former in an unsupervised fashion and only optimizing the latter on account of training data. Crucially, this leads to significantly smaller training times for the supervised matching task and, consequently, enables the use of the resulting matching model in iterative active learning strategies that seek to assist the user in generating training data. Moreover, the feature engineering task in VAER builds on a *representation learning* paradigm [21] that enables the transfer of the resulting representation model to multiple different ER tasks, i.e. transfer learning [22].

In supporting the above characteristics, the techniques used with VAER intersect with the following research areas:

Variational Auto-Encoders. VAEs [8], [23] are a type of neural network often used in dimensionality reduction, representation learning and generative learning. Typically, a VAE involves an *encoder* and a *decoder* that are trained simultaneously. The encoder aims to approximate a (lower dimension) probability distribution of the input using variational inference [24], [25]. The decoder assists the encoder by ensuring that any random sample from the approximated distribution can be used to reconstruct the input. Therefore, VAEs can be seen as unsupervised models, since the labels are the inputs themselves. In this paper, we use a VAE to perform unsupervised

entity representation learning. Formal details about our VAE-based approach are further provided in Section III.

Active Learning. AL is a sub-field of machine learning based on the key hypothesis that if a learning algorithm can suggest the data it learns from, it could perform better with less training [26]. In ER, AL has been used to ease the user’s task of labeling training data (e.g., [7], [27], [28]). For example, [28] offers a framework for AL in ER with various types of non-deep learning algorithms. With respect to deep learning ER, in [7], new training samples are used to adapt a transferred matching model from another ER use-case to the case at hand. While our approach follows a similar methodology, we do not assume pre-trained matching models and start from very few labeled instances to create an, often weak, initial model that is then iteratively improved based on evidence specific to and dictated by the nature of our entity representations.

III. UNSUPERVISED REPRESENTATION LEARNING

With respect to ER feature engineering, we need to convert each input tuple into a numeric vectorized representation expected by downstream matching tasks. The viability of such representations ultimately determines the effectiveness of the entire ER process. Viable representations compact most of the high-level similarity-salient factors into dense vectors that are close together in their multivariate space for duplicates and far apart for non-duplicates. In this section, we set out to generate such representations, albeit in the more expressive form of probability distributions, rather than fixed vectors. Here, we emphasize a *first cost-effectiveness property* of our system: we generate tuple representations unconstrained by the need for training data or user decisions with respect to data characteristics that govern the similarity of two entities.

A. Entity representation architecture

The intuition in this section is that the attribute values of two duplicate tuples were generated from the same (or similar) prior distributions that encode the information conveyed by the said values. We attempt to approximate these attribute-level distributions as Gaussians by using a VAE with *shared parameters* across attributes¹. Note that the distribution type is dictated by the need for analytical interpretation and stability of the optimization function used during training (Section III-C). One other distribution with similar properties is the von Mises–Fisher distribution [29]. However, a sufficiently powerful encoder and decoder (i.e., with non-linearity) can map arbitrary distributions to the Gaussian/von Mises–Fisher and back, so from a theoretical viewpoint, the only constraint for the choice of latent distribution is given by the VAE training process and the smoothness of the latent space [8].

Broadly, given a tuple with m attribute values, $\{A_1, \dots, A_m\}$, for each A_i , we want to approximate a distribution over some random variable which encodes both *morphological* and *semantic* factors. The first step towards

¹By “shared” we mean that the model will generate representations for all attribute values of a tuple simultaneously by processing a 2-d input: *num. attributes* \times *num. features*

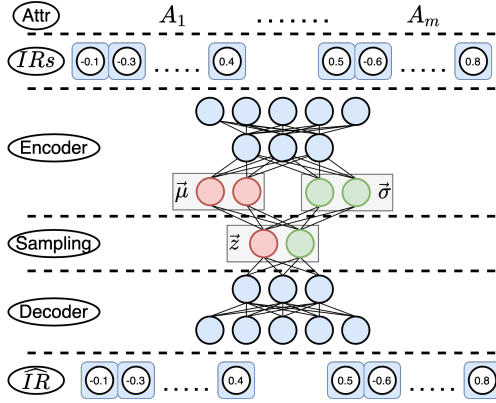


Fig. 2: Proposed entity representation model architecture

this goal is to map individual attribute values to dense vectors, which we call *Intermediate Representations (IRs)*, capable of capturing the similarity between close attribute values. Then, we proceed to approximating a distribution over *IRs* that will allow us to probabilistically reason about their similarity. Assuming for now the existence of *IRs*, Figure 2 illustrates the overall neural architecture of the entity representation model proposed in this paper.

Attr. The attribute values layer where we treat each attribute value independently. Consequently, tuple comparison at matching time can be more granular, i.e., comparing attribute representations pair-wise. Furthermore, attribute-level weighted matching schemes can also be employed.

IR. The Intermediate Representation layer where attribute values are transformed into initial vectorized representations that encode semantic and morphological factors. These representations are the inputs to the VAE and are further described in the next subsection.

Encoder. The encoding layer that takes a collection of *IRs* as input, passes them through one or more *dense* neural layers with *non-linear* activation functions, e.g., rectified linear functions (ReLU), and approximates a latent multivariate Gaussian distribution with diagonal covariance, $\mathcal{N}(\mu, \sigma)$, for each *IR*. The mean and covariance diagonal parameters of distributions produced by the *Encoder*, $\{(\mu_1, \sigma_1), \dots, (\mu_m, \sigma_m)\}$, one for each attribute value, denote the desired entity representations used in downstream tasks to identify duplicates. In other words, each tuple will be represented by a collection of (μ, σ) pairs and the comparison of two tuples will be performed attribute-wise by comparing the corresponding distributions.

Sampling. This layer performs ancestral sampling from each $\mathcal{N}(\mu, \sigma)$ following a procedure specific to VAEs known as the *reparameterization trick* [8]. This allows training a VAE by means of backpropagation with (stochastic) gradient descent [30] that requires the model to be deterministic. Moreover, this step confers a generative property to the representation model: given an attribute value v , each sample z generated from the corresponding $\mathcal{N}(\mu_v, \sigma_v)$ can faithfully encode the latent characteristics of v .

Decoder. The decoding layer that reverses the encoding to reconstruct the original input (i.e., *IRs*), conditioned by latent variables z randomly sampled from $\mathcal{N}(\mu, \sigma)$.

\widehat{IR} . The last layer of the architecture denotes the reconstructed *IRs* that, ideally, are as close as possible to the original *IRs*. The difference between the input *IRs* and the output \widehat{IRs} represents one of the minimizing objectives used in training the model, as described in Section III-C.

Given a collection of *IRs*, the components described above are trained in tandem. Before describing this training process we first discuss how we obtain *IRs* and their importance.

B. Intermediate representations of attributes

Deep-learning models, including VAEs, operate on numerical inputs, i.e., feature vectors. Therefore, we need to convert attribute values into such numerical vectors to be used with our VAE. In this paper, we rely on a simple method based on topic modeling techniques to generate these *intermediate representations (IR)*. Topic modeling assumes that the semantics of a document, or attribute value in our case, is being governed by some unseen (i.e., latent) topics that can be extracted and used as summarizing representations [31]. Examples of methods for generating topical *IRs* include Latent Semantic Analysis (LSA) [32] or Latent Dirichlet Allocation [33]. In practice, LSA has proven more efficient with similar effectiveness and we use it to generate topical *IRs* by extracting latent topics per attribute value. Concretely, the corpus of all attribute values is considered for topic extraction using LSA, with each value being construed as a document. This results in a topic vector for each attribute value, i.e., the inputs to the *Encoder* layer in Figure 2. Note that, since LSA and topic modeling are commonly used on categorical data, in this paper we focus on data that is either categorical or its numerical values can be treated as words, e.g., phone numbers.

An alternative to topical *IR* extraction is *distributed IR* extraction, based on word-embedding models (e.g., [6], [34], [35]). These have been successfully used in NLP (e.g., [4], [36]), data discovery (e.g., [37]), or entity resolution (e.g., [2], [3]). In practice, we observed that distributed *IRs* lead to similar effectiveness to topical *IRs*, with the additional overhead of manipulating large pre-trained embeddings. Therefore, in this paper, we only rely on topical *IRs*.

IRs are important because they encode morphological and semantic information of values. Without their use, we would have to rely on the VAE architecture to learn numerical representations of words (using deep *Embedding* layers). This would require large training times and training corpora. Furthermore, *IRs* enable a transferability property of the representation learning model, as later discussed in Section III-D. Therefore, by using *IRs*, we further contribute to cost reductions of the ER process by (i) reducing the dimensionality of the VAE; (ii) speeding up the VAE training process or omitting it altogether through transfer learning; and (iii) reducing the generalization requirements, since part of the similarity correlations between words aimed to be conveyed by the final representations are already caught by *IRs*.

C. Learning entity representations: training the VAE

IRs can themselves act as entity representations. However, they are deterministic, fixed vectors in a potentially irregular latent space with reduced control over how close duplicates end up. In practice, *IRs* tend to be effective for clean and structured data and less so when data is dirty. The model from Figure 2 attempts to address such limitations by learning a probabilistic model over *IRs*. Specifically, it encodes a given input, *IR* in our case, as a probabilistic latent variable z that captures the high-level information of the input, and then decodes that input (or a close version of it) from z . The objective of the encoding-decoding process is to minimize the error between the input and the output [8].

More formally, given a collection of n entities with m attributes and each entity represented by the m *IRs* of its attribute values, $\{\{IR_1^1, \dots, IR_m^1\}, \dots, \{IR_1^n, \dots, IR_m^n\}\}$, we consider each *IR* to be a random variable generated by some random process involving a lower-dimension latent variable z drawn from some prior distribution $p(z)$ that conveys high-level similarity-salient factors of *IR*. We want to infer the characteristics of z , given *IR*. In other words, we want to compute a posterior distribution $p(z|IR)$, given by $p(z|IR) = \frac{p(IR|z)p(z)}{p(IR)}$. Computing the denominator $p(IR) = \int p(IR|z)p(z)dz$ is intractable due to the multidimensionality of *IR* and z [8]. Alternatively, $p(z|IR)$ can be approximated through *variational inference* [25] by another tractable (e.g., Gaussian) distribution $q(z|IR)$. In practice, this translates to minimizing the Kullback–Leibler (KL) divergence between $q(z|IR)$ and $p(z|IR)$ which can be achieved by maximizing the following [8]:

$$\mathbb{E}_{q(z|IR)} \log(p(IR|z)) - KL(q(z|IR)||p(z)) \quad (1)$$

where the first term represents the *expected log-likelihood* of faithfully reconstructing *IR* given some z from $q(z|IR)$, and the second term is the KL divergence between our approximated distribution $q(z|IR)$ and the true prior. Consistently with our initial assumption, Equation 1 ensures that $q(z|IR)$ describes a distribution of faithful latent representations of *IR*, so that *IR* can be reconstructed from its samples, and that any latent representation z comes from a similar distribution to the assumed prior $p(z)$. In practice, by fixing $p(z) = \mathcal{N}(0, I)$ (i.e., the standard normal distribution of mean 0 and diagonal unit covariance), the VAE enforces a regular geometry on the latent space so that similar data lead to similar latent variables [38].

From a practical perspective, we can construct the inference model described above into a neural network model where a function $\phi : \mathbb{R}^d \rightarrow \mathbb{R}^k$, i.e., our *Encoder* from Figure 2, maps a d -dimensional input, *IR*, to two k -dimensional variables, μ and σ , denoting the parameters of a latent Gaussian distribution, $q_\phi(z|IR)$. Additionally, a second function, $\theta : \mathbb{R}^k \rightarrow \mathbb{R}^d$, i.e., our *Decoder* from Figure 2, ensures that any latent variable z sampled from $q_\phi(z|IR)$ can be used to produce an approximate reconstruction of *IR*, (i.e., \widehat{IR}). The loss function minimized in learning the parameters of ϕ and θ

follows the relation from Equation 1, extended to include all m *IRs* (i.e., attribute values) of a tuple:

$$\begin{aligned} L_{(\phi, \theta)}(IR, \widehat{IR}) &= \sum_{i=1}^m \mathbb{E}_{q_\phi(z_i|IR_i)} [\log(p_\theta(IR_i|z_i))] \\ &\quad - \sum_{i=1}^m KL(q_\phi(z_i|IR_i)||\mathcal{N}(0, I)) \end{aligned} \quad (2)$$

Intuitively, by fitting the inputs to Gaussian distributions, the VAE learns representations of attribute values not as single points, but as ellipsoidal regions in the latent space, forcing the representations to continuously fill this space. Specifically, the mean μ of the latent distribution controls where the encoding of an input should be centered around, while the diagonal covariance σ controls how far from the center the encoding can vary. As decoder inputs are generated at random from anywhere inside this distribution (recall the *Sampling* layer of Figure 2), the decoder is exposed to a range of variations of the encoding of the same input during training. The decoder, therefore, learns that, not only is a single point in the latent space referring to an attribute value, but all nearby points refer to that value as well, i.e., accounting for variation and uncertainty across the attribute values of duplicates.

Lastly, by learning independent representations for each attribute value, we obtain *disentangled* representations of tuples, $\{(\mu_1, \sigma_1), \dots, (\mu_m, \sigma_m)\}$. By disentangled, we mean a representation where single latent units (e.g., (μ_i, σ_i)) are sensitive to changes in single attribute values, while being relatively invariant to changes in other attribute values.

D. Representation model transferability

The architecture from Figure 2 enables a representational property which we emphasize as a *second cost-reduction characteristic* to our overall approach: the representation model trained during one ER task can be reused in other ER tasks, therefore eliminating the need for representation learning. In other words, the architecture from Figure 2 allows for transfer learning [22]. This is by virtue of the variational inference and the use of *IRs* as inputs. Concretely, the VAE from Figure 2 learns how to encode multi-dimensional numerical inputs, i.e., *IRs*, into latent distributions, and to decode samples from the said distributions back to their corresponding inputs by splitting the latent space into ellipsoidal regions that allow for variation across *IRs*. Once the parameters of the VAE are trained, any new *IR* with *similar dimensionality and scale* has the potential of being accurately encoded/decoded by the model, regardless of the *IR*'s data domain. The representation model is, therefore, *domain agnostic*. It follows that the transferability property can eliminate the need for feature engineering when performing ER tasks on new datasets. Consequently, it minimizes the training-time cost of our overall ER solution (as shown in Section VI), since representation learning accounts for most of the training time needs.

TABLE I: Duplicate candidates songs example

Song	Artist	Album	Year
Charlie Brown	Coldplay	Mylo Xyloto	2011
Charlie Brown	Coldplay	GRAMMY Nominees	2013

IV. SUPERVISED MATCHING IN THE LATENT SPACE

The transferability property of our proposal is complemented by an adaptability property. Specifically, the representations produced by the model from Figure 2 are lenient with respect to small variations in the attribute values of two duplicate tuples. However, more significant discrepancies between duplicates that are not reflected in the *IRs* can lead to far apart latent distributions, especially if the representation model has been transferred from another use-case. Moreover, since the representation learning step is unsupervised, the notion of similarity between tuples conveyed by the learned representations may not be consistent with the real intended notion. For instance, consider the example from Table I. Both entities denote the same song by the same artist released as part of two different albums. Whether or not the two tuples are duplicates depends on the use-case and the unsupervised representations may not reflect that decision. There is, therefore, a need for (i) adjusting the entity representations to cover more significant discrepancies between duplicates, and (ii) aligning the notion of similarity conveyed by the representations with the use-case intent, i.e., similarity learning. In this section, we describe our supervised deep learning proposal for addressing these requirements.

A. Matching architecture

In Section III we focused on a *generative* task of producing similarity-preserving entity representations. We now describe a *discriminative* task that builds on the generative model to learn a similarity measure between representations and to perform ER matching. More specifically, given a set of tuple pairs (s, t) , each with m attribute values $\{A_1^s, \dots, A_m^s\}$ and $\{A_1^t, \dots, A_m^t\}$, and corresponding duplicate/non-duplicate labels, we perform supervised training of a Siamese neural network (i.e., a class of neural network that contain two or more identical sub-networks) [9], [39]. Our proposed architecture is illustrated in Figure 3.

Attr and **IR**. These layers correspond to the first two layers from Figure 2: each attribute value of the input tuples is mapped to an *IR* which is then passed to the next layer.

Encoder. This layer uses two variational encoders, similar to the one from Figure 2. Both encoders share the same weights initialized with the trained values of the variational encoder in Figure 2. Parameter updating is mirrored across both encoders during training and each encoder generates an entity representation, $\{(\mu_1^s, \sigma_1^s), \dots, (\mu_m^s, \sigma_m^s)\}$, corresponding to its input tuple. The purpose of this layer is to improve the weights transferred from the variational encoder of the representation model on account of training data.

Distance. Modeling the latent space using probability distributions allows us to reason about the similarity of s and t in terms

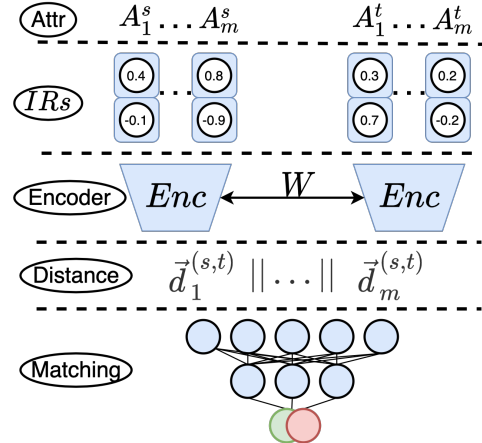


Fig. 3: Proposed matching model architecture

of the distance between their corresponding distributions. Two examples of metrics that can be used to quantify such distance between Gaussian distributions are Wasserstein [40] and Mahalanobis [41]. These have previously been used in learning sentence similarity in NLP (e.g., [42]). In practice, both distances showed similar effectiveness, so we are only discussing the former here.

Intuitively, the d -Wasserstein distance quantifies the minimal cost of transporting the unit mass of one probability measure into the unit mass of another probability measure, when the cost is given by an L^d distance [40]. In our case, we consider $d = 2$ and the squared 2-Wasserstein distance (W_2^2) between two k -dimensional diagonal Gaussian distributions, p and q , is given by Equation 3.

$$W_2^2(p, q) = \sum_{i=1}^k (\mu_i^p - \mu_i^q)^2 + (\sigma_i^p - \sigma_i^q)^2 \quad (3)$$

Returning to the *Distance* layer in Figure 3, from the two inputs $\{(\mu_1^s, \sigma_1^s), \dots, (\mu_m^s, \sigma_m^s)\}$ and $\{(\mu_1^t, \sigma_1^t), \dots, (\mu_m^t, \sigma_m^t)\}$, we compute m attribute-wise Wasserstein distance vectors $\vec{d}^{(s,t)} = (\mu^s - \mu^t)^2 + (\sigma^s - \sigma^t)^2$. Finally, we concatenate all m distance vectors and pass the result to the next layer.

Matching. This layer performs ER matching in the form of a binary classification task. The classifier consists of a two-layer Multi Layer Perceptron (MLP) with non-linear activation functions that, given the m concatenated Wasserstein distance vectors, predicts a match/non-match label. The purpose of this layer is to discriminate between duplicates and non-duplicates.

Given training data, the model from Figure 3 undergoes a training process based on backpropagation and (stochastic) gradient decent, with the weights of *Matching* and *Encoder* layers being updated at each step, as we now describe.

B. Learning entity similarity: training the Siamese network

The training process of the proposed matching model involves two optimization objectives: (1) minimize the W_2^2 distance between the representations of duplicates and maximize it for non-duplicates, i.e., improving the *Encoder* layer, and

(2) minimize the classification error of the binary classifier, i.e., training the *Matching* layer. These two objectives are optimized simultaneously. Firstly, with respect to (1), we further improve the initial weights of the Siamese encoder heads on account of training data so that they are consistent with more complex cases of tuple similarity, infeasible to cover by the unsupervised approach alone. Secondly, in relation to (2), we optimize the parameters of the binary classifier such that the resulting model is effective in discriminating between duplicate and non-duplicate tuples. To this end, we use a contrastive loss function [39] defined by Equation 4:

$$\begin{aligned} L(s, t) = & y \log(p_\gamma(y|d^{(s,t)})) + (1-y) \log(1-p_\gamma(y|d^{(s,t)})) \\ & + \frac{1}{m} \sum_{i=1}^m [x W_2^2(q_\phi(A_i^s), q_\phi(A_i^t)) \\ & + (1-x) \max(0, M - W_2^2(q_\phi(A_i^s), q_\phi(A_i^t)))] \end{aligned} \quad (4)$$

where y is the predicted class for a pair of tuples (s, t) , x is the true class, $p_\gamma(y)$ is the predicted probability of y , γ are the parameters of the binary classifier, $d^{(s,t)}$ is the distance vector from the *Distance* layer in Figure 3, $q_\phi(A_i^j)$ is the Gaussian distribution approximated for attribute A_i^j by the encoding layer, and ϕ are the parameters of the encoders. M is a margin hyperparameter that controls how the encoders weights are adjusted in light of the training data.

The first term in Equation 4, i.e., the cross-entropy of the prediction, covers objective (2) from above, while the second term covers objective (1). The function of the margin M is that, when the representations produced for a negative pair are distant enough, no effort is wasted on maximizing that distance, so further training can focus on more difficult pairs.

The cost benefits of the feature and similarity learning approaches described in Sections III and IV are now clear: given two input tables (as in Figure 1), the unsupervised representation learning model from Figure 2 alleviates the user from deciding on the features that govern the tuple comparison process, and from providing training data to generate those features. The potential loss in feature expressiveness determined by the unsupervised nature of the representation model, or by the use of a transferred representation model, is attenuated by the Siamese matching model from Figure 3 that adjusts the parameters of the representation encoder in light of training data. This adjustment is also efficient, since most of the optimization work has already been done by the unsupervised training process.

V. ACTIVE LEARNING IN THE LATENT SPACE

Deep learning solutions are often characterized by the need for a significant number of training instances (e.g., up to thousands [3]). Active learning (AL) [26] has traditionally been proposed to support the manual labeling of such volumes where an initial pool of labeled instances, \mathcal{L} , and a much larger pool of unlabeled instances, \mathcal{U} , are assumed. Then, the user is tasked with labeling one or more instances from \mathcal{U} to iteratively update \mathcal{L} . The crux of an AL strategy is the sampling method used to choose instances from \mathcal{U} to be passed

Algorithm 1 AL bootstrapping

Input: Tuples T , repres. model ϕ , num. neighbours k
Output: Pos/Neg/Unlabeled tuple pairs $\mathcal{L}^+/\mathcal{L}^-/\mathcal{U}$

```

1: function ALBOOTSTRAP
2:    $\mathcal{U} \leftarrow \{\}$ 
3:    $R \leftarrow \phi.\text{predict}(T)$ 
4:    $I \leftarrow \text{Ish\_index}(R)$ 
5:   for all  $t_i \in T$  and  $r_i \in R$  do
6:      $N = I.\text{lookup}(r_i, k)$ 
7:     for all  $n_j \in N$  do
8:        $\mathcal{U} \leftarrow \mathcal{U} \cup \{(t_i, n_j)\}$ 
9:     end for
10:   end for
11:    $W_{min} = \min_{(s,t) \in \mathcal{U}} W_2^2(\phi(s), \phi(t))$ 
12:    $W_{max} = \max_{(s,t) \in \mathcal{U}} W_2^2(\phi(s), \phi(t))$ 
13:    $\mathcal{L}^+ \leftarrow \{(s, t) | (s, t) \in \mathcal{U}, W_2^2(\phi(s), \phi(t)) \approx W_{min}\}$ 
14:    $\mathcal{L}^- \leftarrow \{(s, t) | (s, t) \in \mathcal{U}, W_2^2(\phi(s), \phi(t)) \approx W_{max}\}$ 
15:   return  $\mathcal{L}^+, \mathcal{L}^-, \mathcal{U} \setminus (\mathcal{L}^+ \cup \mathcal{L}^-)$ 
16: end function

```

to the user for labeling. Many such strategies proposed for various learning algorithms (e.g., [28]) often degenerate to random sampling or to sampling from a single class when used with highly stochastic models such as neural networks [43], [44]. Furthermore, the computational overhead of training deep neural networks precludes approaches that expect model retraining over many iterations.

In this section, we propose an AL sampling strategy facilitated by the decoupling of feature and matching learning tasks and by VAE’s latent space. This strategy is characterized by three important properties:

- **Class balance:** ensures that the samples presented to the user for labeling represent both matches and non-matches and, thus, avoids class imbalance problems.
- **Informativeness:** ensures that the samples presented to the user for labeling maximize the information gain and, thus, potentially speed up the matcher generalization.
- **Diversity:** ensures that the samples selected for user labeling cover a diversified range and, thus, prevents overfitting.

Here we emphasize a *third cost-effectiveness property* of our proposal: decoupling the matching model reduces training times to an extent that enables iterative training over multiple active learning iterations using a proposed sampling strategy that eases the manual task of labeling data, as we now describe.

A. Bootstrapping for initial training data

Contrary to previous deep ER-specific AL approaches (e.g., [7]), in this paper we aim to automatically create the initial pool of labeled instances \mathcal{L} , factored as two disjoint subsets, $\mathcal{L}^+ \cup \mathcal{L}^- = \mathcal{L}$, for matches and non-matches, respectively. To this end, we use Algorithm 1 that relies on the latent space, modeled as described in Section III, to identify the nearest and the furthest entity representations to act as initial positive and negative examples, respectively.

Specifically, given a collection of input tuples, T , and a representation model ϕ , trained as described in Section

III, we first generate the pool of unlabeled candidates, \mathcal{U} , by performing nearest-neighbour search, e.g., using Locality Sensitive Hashing [45] with Euclidean distance [46], (Lines 3–10), i.e., each candidate is a pair of neighboring tuples (s, t) that may or may not be duplicates. Note that the use of LSH based on Euclidean distance is possible because, looking back to Equation 3, we observe that the W_2 distance of two k -dimensional Gaussian distributions $p = \mathcal{N}(\mu^p, \sigma^p)$ and $q = \mathcal{N}(\mu^q, \sigma^q)$ is *positively correlated* with the squared Euclidean distance of their means, given by $\sum_{i=1}^k (\mu_i^p - \mu_i^q)^2$. In other words, duplicate tuples that have W_2 -close representations in the latent space will have Euclidean-close means as well. This observation allows us to use the Euclidean distance as surrogate for similarity candidates and employ LSH algorithms to efficiently find them.

Next, we measure the distances between the closest and the furthest two neighbours in \mathcal{U} using Equation 3 and use them as approximate thresholds for initial positive and negative samples (Lines 11, 12). The sets of positive (i.e., \mathcal{L}^+) and negative (i.e., \mathcal{L}^-) samples are given by pairs with similar distances between their members to the minimum and maximum distances, respectively (Lines 5, 6).

The intuition behind Algorithm 1 is that very similar tuples will end up with very small distances between their representations and we can automatically choose them as initial positive samples. Similarly, tuples that are very far apart will be easily identified by their distance and automatically chosen as initial negative samples.

B. Sampling for AL in the latent space

Having obtained initial \mathcal{L}^+ , \mathcal{L}^- and \mathcal{U} , we now describe how we aim to iteratively improve these sets through a sampling strategy that exhibits the three properties mentioned at the beginning of this section.

1) *Class balance*: Given the unlabeled pool \mathcal{U} , in reality only very few of its instances are positives, while the vast majority are negatives. We therefore need to ensure sampling from both categories. We do so by treating positive and negative candidates separately and discriminate between them using the matching model γ , trained on $\mathcal{L}^+ \cup \mathcal{L}^-$ as described in Section IV. Specifically, instead of sampling from \mathcal{U} , we sample from each $\mathcal{U}^+ = \{(s, t) | (s, t) \in \mathcal{U}, p_\gamma(1 | (s, t)) > 0.5\}$ and $\mathcal{U}^- = \{(s, t) | (s, t) \in \mathcal{U}, p_\gamma(1 | (s, t)) \leq 0.5\}$, where $p_\gamma(1 | (s, t))$ is the probability of a given sample (s, t) to be a positive under the current matching model γ for that iteration.

2) *Informativeness*: Given the unlabeled pool \mathcal{U} , AL theory hypothesizes that there is a sub-set in \mathcal{U} of minimal size that offers maximum generalization power to a matching model. We therefore need to get as close as possible to this sub-set in order to maximize the information gain of the resulting model. We do so by using one of the most common measures for the amount of information carried by a potential training sample: the *entropy* of the conditional probability under the model aimed to be improved [26]. More formally, given γ and $\mathcal{U} = \mathcal{U}^+ \cup \mathcal{U}^-$, we can use the entropy measure, given by

Equation 5 for the binary case, to choose the most informative instances in \mathcal{U} to be labeled by the user.

$$H_\gamma(s, t) = -p_\gamma(y | (s, t)) \log(p_\gamma(y | (s, t))) + (1 - p_\gamma(y | (s, t))) \log(1 - p_\gamma(y | (s, t))) \quad (5)$$

where y is the predicted class for a tuple pair $(s, t) \in \mathcal{U}$ and $p_\gamma(y | (s, t))$ is the predicted probability of y under the current model γ .

Intuitively, $H(s, t)$ is high for pairs of uncertain tuples whose probability of being duplicate/non-duplicate is close to 0.5, and low otherwise. Therefore, in our sampling strategy, those (s, t) from \mathcal{U} that have a high entropy are most informative to the model.

3) *Diversity*: Given the unlabeled pool \mathcal{U} , in addition to entropy, we also have to consider the distance between the tuple representations of each instance. This is because treating positives and negatives separately is often not enough to ensure class balance, i.e., many of the predicted positives with high entropy are in reality negatives. We therefore sample positive candidates that have a high positive probability and a distance between their tuple representations similar to the distances associated with samples from \mathcal{L}^+ . However, most of the initial \mathcal{L}^+ constituents have very small distances between their tuples. Consequently, the Wasserstein vectors computed in the *Distance* layer of Figure 3 will be similar, if not identical. We therefore need to ensure that the AL sampling strategy chooses more diverse positive candidates. We do so by considering the entire distribution of distances between tuple representations of members of \mathcal{L}^+ . More specifically, given a set of duplicates \mathcal{L}^+ and a representation model ϕ , we repeatedly sample from each $\phi(s)$ and $\phi(t)$, with $(s, t) \in \mathcal{L}^+$, using the *Sampling* step from Figure 2, i.e., VAE’s *reparameterization trick* [8], to obtain a distribution of possible Euclidean distances D^+ between duplicate representations, as shown in Equation 6.

$$D^+ = \{\|z_i^s - z_i^t\|_2 | (s, t) \in \mathcal{L}^+, s_i \in \text{sampling}(\phi(s)), t_i \in \text{sampling}(\phi(t))\} \quad (6)$$

Recall that, given a trained variational encoder ϕ , every sample from the approximated distribution for a tuple t produced by $\phi(t)$ can act as a viable encoding from which the input can be decoded. Therefore, by repeatedly sampling from each $\phi(s)$ and $\phi(t)$, with $(s, t) \in \mathcal{L}^+$, Equation 6 produces a distribution of possible distances between duplicate representations².

Having obtained D^+ , we can employ Kernel Density Estimators (KDE) [47] using Gaussian kernels to estimate a univariate probability density function, $\hat{f}^+(d)$, over all distances $d \in \mathcal{D}^+$. Then, $\hat{f}^+(d)$ can be applied on the distances between tuple representations of each unlabeled instance from \mathcal{U} to identify the ones that are most likely to be positives, and use this information in addition to entropy.

²We need to repeatedly sample, e.g., 1000 samples for each tuple, because \mathcal{L}^+ alone often contains insufficient samples to accurately estimate the distance distribution.

Algorithm 2 AL for ER

Input: Tuples T , repres. model ϕ , num. iterations I , num. neighbours k

Output: Matching model γ

```

1: function AL
2:    $\mathcal{U}, \mathcal{L}^+, \mathcal{L}^- \leftarrow \text{ALBOOTSTRAP}(T, \phi, k)$ 
3:    $\gamma \leftarrow \text{train}(\mathcal{L}^+, \mathcal{L}^-)$ 
4:    $\hat{f}^+(d) \leftarrow \text{KDE}(\mathcal{L}^+)$ 
5:   for all  $i \in I$  do
6:      $c^+ \leftarrow (s, t), \min_{(s,t) \in \mathcal{U}^+} H_\gamma((s, t)) \times \frac{1}{\hat{f}^+(d((s, t)))}$ 
7:      $c^- \leftarrow (s, t), \min_{(s,t) \in \mathcal{U}^-} H_\gamma((s, t)) \times \hat{f}^+(d((s, t)))$ 
8:      $u^+ \leftarrow (s, t), \min_{(s,t) \in \mathcal{U}^+} \frac{1}{H_\gamma((s, t))} \times \hat{f}^+(d((s, t)))$ 
9:      $u^- \leftarrow (s, t), \min_{(s,t) \in \mathcal{U}^-} \frac{1}{H_\gamma((s, t))} \times \frac{1}{\hat{f}^+(d((s, t)))}$ 
10:     $\text{label}(c^+); \text{label}(c^-); \text{label}(u^+); \text{label}(u^-)$ 
11:     $\mathcal{L}^+ \leftarrow \mathcal{L}^+ \cup \{c^+, u^+\}; \mathcal{L}^- \leftarrow \mathcal{L}^- \cup \{c^-, u^-\}$ 
12:     $\mathcal{U} \leftarrow \mathcal{U} \setminus (\mathcal{L}^+ \cup \mathcal{L}^-)$ 
13:     $\gamma \leftarrow \text{train}(\mathcal{L}^+, \mathcal{L}^-)$ 
14:     $\hat{f}^+(d) \leftarrow \text{KDE}(\mathcal{L}^+)$ 
15:   end for
16:   return  $\gamma$ 
17: end function

```

4) *Balanced, informative and diverse sampling*: Algorithm 2 unifies all the steps discussed in this section. Specifically, once the initial sets of unlabeled/labeled samples have been generated (i.e., *Line 2*), the initial matcher trained (i.e., *Line 3*), and the initial positive probability density function estimated (i.e., *Line 4*), we iteratively proceed as follows:

Certain positives. We identify duplicate candidates with low entropy and high distance likelihoods as certain positives (i.e., *Line 6*). Intuitively, these are instances characterized by a high positive probability under the current model and a distance value between their representations *similar* to the distances associated with \mathcal{L}^+ .

Certain negatives. We identify non-duplicate candidates with low entropy and low distance likelihood as certain negatives (i.e., *Line 7*). Intuitively, these are instances characterized by a high negative probability under the current model and a distance value between their representations *dissimilar* to the distances associated with \mathcal{L}^+ .

Uncertain positives. We identify duplicate candidates with high entropy and low distance likelihood as uncertain positives (i.e., *Line 8*). Intuitively, these are instances characterized by a low positive probability under the current model (although higher than 0.5) and a distance value between their representations *dissimilar* to the distances associated with \mathcal{L}^+ .

Uncertain negatives. We identify non-duplicate candidates with high entropy and high distance likelihood as uncertain negatives (i.e., *Line 9*). Intuitively, these are instances characterized by a low negative probability under the current model (although higher than 0.5) and a distance value between their representations *similar* to the distances associated with \mathcal{L}^+ .

Algorithm 2 identifies two types of samples for each class, *viz.* certain and uncertain. Uncertain samples have high infor-

TABLE II: Datasets used in the experiments

Domain	Card.	Arity	Training	Test
Restaurants [†]	533/331	6	567	189
Citations 1 [†]	2616/2294	4	7417	2473
Citations 2 [†]	2612/64263	4	17223	5742
Cosmetics [‡]	11026/6443	3	327	81
Software [‡]	1363/3226	3	6874	2293
Music [‡]	6907/55923	8	321	109
Beer [‡]	4345/3000	4	268	91
Stocks [‡]	2768/21863	8	4472	1117
CRM [†]	5742/9683	12	440	220

mative value for the model since they are close to the decision boundary (i.e., high entropy) and have surprising distances between their tuple representations given their predicted class. Conversely, the purpose of certain samples is to prevent overfitting to the selected uncertain instances. Finally, in Algorithm 2, user involvement is only required at *Line 10* and, although Algorithm 2 assumes sampling one instance of each type per iteration, in practice the algorithm can easily be extended to perform batch sampling by choosing the top- k instances at each of *Lines 6,7,8,9*.

VI. EVALUATION

In this paper we set out to decrease the cost associated with ER tasks, and approached this by decoupling feature learning from matching tasks. In this section, we empirically show that this decoupling contributes to the cost reduction desideratum without compromising effectiveness.

A. Experimental setup

1) *Datasets*: We conduct experiments on nine datasets from eight domains. Table II shows an overview of the evaluation data used in this section. Each domain (i.e., **Domain** column) presents two tables (of **Card.** cardinality) between which we aim to perform ER, with the same **Arity** and aligned attributes. Each domain also comes with a training set with duplicate and non-duplicate example pairs (of **Training** size), and a similar, albeit smaller, test set (of **Test** size).

Datasets marked with [†] are *clean* with few missing values. Datasets marked with [‡] are *noisy* and more challenging to perform ER on due to their many missing values and unstructured attributes, e.g., product descriptions. Finally, the first seven domains have been previously used in ER benchmarks (e.g., [2], [3]), while the last two are private datasets from *Peak AI* with data about clothing products and person contacts.

2) *Baselines and reported measures*: We build our evaluation around *Precision* (P), *Recall* (R) and *F-measure* ($F1$), measured on the test datasets. For the purposes of computing these measures, we define a true positive (tp): any pair of tuples marked as duplicate in both the test set and the evaluated results; a false positive (fp): any pair of tuples marked as non-duplicate in the test set and as a duplicate in the evaluated results; and as a false negative (fn): any pair of tuples marked as a duplicate in the test set and as a non-duplicate in the evaluated results. Then, $P = \frac{tp}{tp+fp}$; $R = \frac{tp}{tp+fn}$; $F1 = 2 * \frac{P \times R}{P + R}$.

TABLE III: Hyperparameters of VAER

Component	Parameter	Value
Repr. learning	IR dimension [†]	300
	VAE latent dimension	100
Matching	Margin $M^†$	1
AL	Samples/iteration	10
AL	Top neighbours $K^†$	10
Repr. learning & matching	Optimizer	Adam
	Learning rate	0.001

TABLE IV: VAER representation learning results

Domain	$P_T@K = 10$		$R_T@K = 10$		$F1_T@K = 10$	
	Unsup	Sup	Unsup	Sup	Unsup	Sup
Restaurants	0.17	0.2	1	1	0.26	0.32
Citations 1	0.45	0.54	0.99	1	0.62	0.7
Citations 2	0.58	0.63	0.93	0.93	0.72	0.75
Cosmetics	0.52	0.5	0.84	0.86	0.65	0.64
Software	0.22	0.32	0.87	0.87	0.35	0.48
Music	0.69	0.7	0.83	0.83	0.76	0.75
Beer	0.37	0.39	0.93	0.93	0.53	0.55
Stocks	0.99	0.99	0.72	0.94	0.84	0.97
CRM	0.97	0.97	0.97	0.98	0.97	0.97

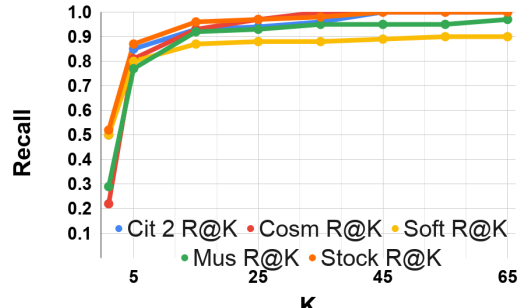
Intuitively, P measures the ability of the evaluated component not to mislabel true negatives, and R measures the ability of the evaluated component to find all the positive test samples.

We consider *DeepER* (*DER*) [2] and *DeepMatcher* (*DM*) [3] as the state-of-the-art in *deep learning* *ER* and configure these systems as described in [3] for the *RNN* (equivalent to *DER*) and *Hybrid* (for *DM*) setups. Other *ER* proposals, such as *Magellan* [16], do not rely on deep learning and have already been subject to extensive comparison against this space [3]. Finally, more recent systems such as *ZeroER* [19], are unsupervised and do not allow for learning a similarity function suitable for the case at hand or for active learning. Therefore, we do not consider unsupervised methods as baselines.

3) *VAER configuration*: Being a deep learning solution, *VAER* requires parameter configuration. Table III shows the values used for the most important *VAER* parameters. The *IR* dimension, the number of neighbors K , and the margin M of the loss function discussed in Section IV are data dependent. However, the values shown in the table led to good results for all the domains used in the evaluation. Lastly, all experiments have been run using *PyTorch* on a *Python 3 Google Compute Engine Backend* with *12 GB RAM* and *GPU acceleration*.

B. Representation learning experiments

In this subsection we evaluate the similarity-preserving nature of our entity representations in both unsupervised and supervised settings. Concretely, we perform LSH-based nearest-neighbor search on representations generated by the encoding layer of Figure 2 (i.e., unsupervised) and by the encoding layer of Figure 3 (i.e., supervised), hypothesizing that *if tuple representations are similarity-preserving, the representations of duplicates will be close by in the latent space and, therefore, deemed near neighbors*. We note that

Fig. 4: Recall@ K as K increases

such an approach can also act as a *blocking* step in an end-to-end *ER* process (similar to [2]) and, therefore, aim for *high recall* because missed duplicates at this step would be unrecoverable by downstream steps, e.g., matching.

Table IV shows the values for precision, recall and F1 score @ $K=10$, indicating that, for each tuple pair in the test set, we measure the effectiveness against the top-10 most similar neighbours of either of the two tuples in the pair.

The **Unsup** columns show the results obtained when performing nearest-neighbour search on the unsupervised representations, i.e., the outputs of the variational encoder. Overall, the recall values are above 85% for most of the domains. In the case of *Cosmetics* and *Music*, there are many similar entities that only diverge in one attribute, e.g., *color*, *release year*. The representations of such tuples tend to be very similar, which leads to slightly lower recall values. The lowest recall value, i.e., for *Stocks*, is determined by noisy data. For example, consider a pair of duplicate descriptions of clothing articles from *Stocks*: (Junior small logo swim short, Jun SML L - white swim srt). This is a representative example of cases we aim to cover by taking training data into account.

The **Sup** columns show the measurements when training data is used to improve the unsupervised representation model parameters, as described in Section IV. The highlighted values show increases in recall, with the *Stocks* case clearly showing the potential benefit of performing supervised improvement of an unsupervised initial representation model.

The effectiveness of the nearest-neighbor search depends on the value of K . Figure 4 shows that most of the cases that did not already achieve good recall in Table IV can be improved by increasing K . The exception, *Software*, is determined by the many missing values existing in the two datasets.

The experiments from this subsection show that our proposed unsupervised representation learning method is *cost-effective* in the sense that it alleviates the user from deciding on the features that govern the similarity between representations and (as we show next) matching-specific comparisons.

C. Supervised matching experiments

In this section, we evaluate the effectiveness and the efficiency of the supervised matching task, hypothesizing that *our proposed matching model is more efficient than other*

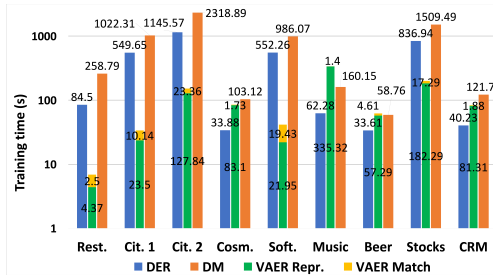


Fig. 5: Training times (s)

deep learning ER approaches, e.g., *DeepER* (DER) and *DeepMatcher* (DM), without compromising effectiveness.

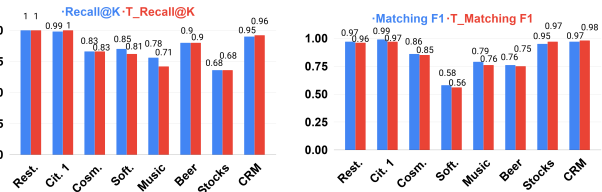
Table V shows the precision, recall and F1 score of the model from Figure 3, of *DeepER*, and of *DeepMatcher*, each trained on given training samples for each of the domains in Table II. The highlighted values denote cases where the results corresponding to our proposed technique achieves better results than the antagonists. However, as with the case when one of the competitors achieves better results, e.g., *Stocks*, the differences are minimal. *Software* is a case of particular interest because it proved problematic for all ER solutions evaluated. This is because its tables contain only three columns, one of which is numerical, one contains software product descriptions that are challenging to compare, and the third presents many missing values.

We can conclude from Table V that our proposed Siamese matching model *achieves state-of-the-art effectiveness levels*. Additionally, the decoupling of feature learning and matching *leads to a significant decrease in training time*, as shown in Figure 5 (note the log scale Y axis). The figure compares the combined training times of VAER’s representation and matching models using topical *IRs* (using distributed *IRs* returns similar results) against *DeepER* and *DeepMatcher*. For five out of nine cases, VAER requires orders of magnitude lower training times. This is by virtue of *IRs* that impose reduced input dimensions, and by virtue of the architectures of the representation and matching models, both of which use simple linear layers, as opposed to complex RNN layers [48]. The other four cases: *Cosmetics*, *Music*, *Beer* and *CRM* are domains with many tuples to deduplicate and reduced amounts of training data. This suggests that VAER’s representation training time is dominated by the size of the input tables, while VAER’s matching training time, similarly to the baselines, is dominated by the size of the training set.

In practice, training representations on large input tables can be accelerated by training on just a sample of all tuples. Alternatively, transfer learning can be employed, as we show in the next experiment.

D. Transferability experiments

Recall that by decoupling the feature and matching learning tasks, VAER enables the transferability of the representation model to other use-cases. In such cases, the representation learning times from Figure 5 are no longer required, making



(a) Blocking Recalls @ $K = 10$

(b) Matching F1 scores

Fig. 6: Blocking Recall and Matching F1 score with local and transferred representation models.

the final training time–cost of VAER dependent only on matching model and, therefore, *drastically smaller than the baselines requirements*. In Figure 6, we further show that the blocking recall @ $K = 10$ and the matching F1 scores *remain mostly unchanged* when the representation model is transferred from another domain, e.g., *Citations 2* in this case (i.e., $T_{Recall@K}$ and $T_{Matching F1}$). We compare this against the results obtained using locally-trained representations, i.e., the representation model is trained on tables of the tested domain (i.e., $Recall@K$ and $Matching F1$). Note that the transferability case restricts the input tables to have the same number of columns expected by the transferred model. Therefore, we only use the first four columns (i.e., the arity of the *Citations 2* domain) of each domain and pad *Cosmetics* and *Software* with one empty column for comparison consistency. This is why the values corresponding to the locally-trained representations are different from the ones in Tables IV and V.

Cases from Figure 6 where the Recall and F1 score of the locally-trained representations are higher, e.g., *Music*, can be explained by the fact that there is more similarity between attribute values of non-duplicates in the tested domain than in the domain used to train the representation model. In practice, a blend of duplicate and non-duplicate tuples from multiple past ER use-cases can be used to create a robust transferable representation model.

Overall, Sections VI-C and VI-D confirm the effectiveness and efficiency of VAER, and the domain agnostic nature of the representation learning task. Together, these characteristics offer a reliable option for using previous representation knowledge and for minimizing the ER training time–cost.

E. Active learning experiments

The practical training times VAER’s matching model exhibit in Figure 5 enable its use in AL schemes where it can be iteratively improved on account of new user-labeled training samples. In this section, we evaluate the cost reduction potential with respect to data labeling of such an AL scheme, i.e., from Section V, hypothesizing that *by actively labeling training samples for the supervised matcher we can still achieve practical effectiveness with less training data*.

Table VI shows the values for the precision, recall, and F1 scores obtained using three types of matching models: a **Bootstrap** matching model trained only on data resulting from Algorithm 1, a **A250** matching model resulting

TABLE V: Similarity learning results showing VAER’s matching effectiveness

Domain	VAER P	VAER R	VAER F1	DER P	DER R	DER F1	DM P	DM R	DM F1
Restaurants	0.94	1	0.97	0.95	1	0.97	0.95	1	0.97
Citations 1	0.97	1	0.99	0.96	0.99	0.97	0.96	0.99	0.98
Citations 2	0.9	0.9	0.9	0.9	0.92	0.91	0.94	0.94	0.94
Cosmetics	0.87	0.94	0.91	0.83	0.96	0.89	0.89	0.92	0.9
Software	0.62	0.64	0.63	0.62	0.62	0.62	0.59	0.64	0.62
Music	0.86	0.86	0.86	0.78	0.9	0.83	0.95	0.81	0.88
Beer	0.75	0.85	0.8	0.59	0.92	0.72	0.63	0.85	0.72
Stocks	0.99	0.99	0.99	1	1	1	0.99	0.99	0.99
CRM	0.97	0.99	0.99	0.96	0.94	0.95	0.98	0.97	0.97

TABLE VI: Active Learning results showing data labeling cost-reductions.

Domain	Precision			Recall			F1				
	Bootstrap	A250	Full	Bootstrap	A250	Full	Bootstrap	A250	Full	F1 %	Training %
Restaurants	0.73	1	0.94	0.6	1	1	0.65	1	0.97	103%	44%
Citations 1	0.96	0.95	0.97	0.84	0.97	1	0.89	0.95	0.99	96%	3.3%
Citations 2	0.9	0.7	0.9	0.33	0.8	0.9	0.48	0.74	0.9	82%	1.4%
Cosmetics [†]	0.67	0.8	0.87	0.91	0.85	0.94	0.77	0.82	0.91	90%	76%
Software	0.25	0.56	0.62	0.41	0.38	0.64	0.31	0.45	0.63	71%	3.6%
Music	0.46	0.8	0.86	0.63	0.83	0.86	0.53	0.81	0.86	94%	76%
Beer [†]	0.51	0.71	0.75	0.55	0.73	0.85	0.52	0.71	0.8	89%	92%
Stocks [†]	0.99	0.95	0.99	0.83	0.85	0.99	0.90	0.89	0.99	90%	5.5%
CRM	0.83	0.78	0.97	0.63	0.88	0.99	0.71	0.82	0.98	84%	56%

from Algorithm 2 with 250 actively labeled samples (i.e., 12 – 13 AL iterations with 10 samples of each uncertain positives/negatives labeled per iteration), and a **Full** matching model trained on all available training data (from Table II). The last two columns denote the percentage of Full model’s F1 score the A250 model achieves and the percentage of Full training data size 250 samples represent. Domains marked with [†] signal cases where the positive samples generated by Algorithm 1 contained false positives that had to be manually removed. On average, Algorithm 1 generated 15 positives and 15 negatives (i.e., a balanced initial training set).

Table VI highlights examples of cases achieving 90% or more F1 score with less actively labeled samples than provided in the training set. Additionally, cases that have a low Bootstrap precision/recall, e.g., *Software*, *Beer* etc., have low diversity in their bootstrap positive/negative instances. This is expected, since Algorithm 1 retrieves the positives/negatives with the lowest/highest distances between their tuples. Cases that show a significant recall increase from Bootstrap to A250, e.g. *Restaurants*, *Citations 2*, *Beer*, confirm the importance of the diversity property for positive instances. Finally, in only one case, the A250 F1 score percentage is smaller than training size percentage, i.e., *Beer*. Here, 250 labeled samples achieved 89% of the F1 score obtained with the 269 samples from the given training set. This is determined by the more diverse positive instances existing in the training data.

Overall, the last two columns of Table VI show that our proposed VAE-based AL strategy *leads to reductions in costs associated with data labeling, while achieving practical effectiveness*. However, the effort required to achieve the Full F1 score with actively labeled data is use-case dependent. Consider Figure 7 where the F1 scores obtained with 250

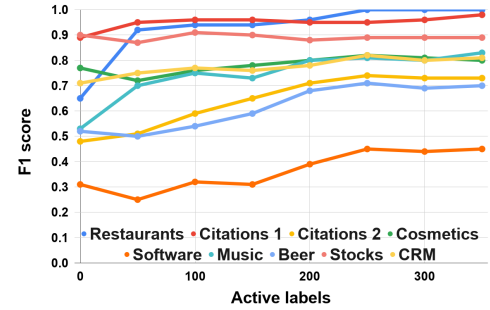


Fig. 7: Active learning F1 score

samples remain unchanged even after 100 additional samples across most of the domains. Continuing the AL iterations for the *Citations 2* domain led to achieving 90% of the Full F1 score with 1050 additional actively labeled samples (i.e., for a total of 7.5% of the training set size). Conversely, for the *Software* domain, the same percentage was achieved with just 400 additional samples (i.e., 9.4% of the training set size).

VII. CONCLUSIONS

In this paper we set out to decrease the cost of performing ER with a deep learning model. We identified three requirements associated with ER in practice that generate user-involvement and time costs: (i) the need for features that capture the similarity between duplicates; (ii) the need for duplicate/non-duplicate example data; and (iii) the need to learn a task-specific discriminative similarity function. We approached the cost-reduction desiderata by decoupling the feature and similarity learning tasks. This decoupling, facilitated by with the use of VAEs for the former, allowed

us to perform *unsupervised* feature engineering, therefore addressing the cost associated with (i); *fast* supervised matching that *adapts* the unsupervised feature space to the ER case at hand, therefore addressing the cost associated with (iii); and active learning on the matching model, therefore addressing the cost associated with (ii). In addition, we showed how *transferring* a representation model across ER use-cases and data domains can further minimize the cost associated with (i). Lastly, we showed that empirical evaluation supports the fulfillment of our cost-reduction desiderata in practice.

VIII. ACKNOWLEDGMENTS

Research supported by a joint collaboration between The University of Manchester, Peak AI Ltd. and Innovate UK as part of a Knowledge Transfer Partnership (KTP11540).

REFERENCES

- [1] P. Christen, *Data Matching - Concepts and Techniques for Record Linkage, Entity Resolution, and Duplicate Detection*, ser. Data-Centric Systems and Applications, 2012.
- [2] M. Ebraheem, S. Thirumuruganathan, S. R. Joty, M. Ouzzani, and N. Tang, “Distributed representations of tuples for entity resolution,” *VLDB*, vol. 11, no. 11, 2018.
- [3] S. Mudgal, H. Li, T. Rekatsinas, A. Doan, Y. Park, G. Krishnan, R. Deep, E. Arcaute, and V. Raghavendra, “Deep learning for entity matching: A design space exploration,” in *SIGMOD*, 2018.
- [4] I. J. Goodfellow, Y. Bengio, and A. C. Courville, *Deep Learning*, ser. Adaptive computation and machine learning, 2016.
- [5] Y. Bengio, R. Ducharme, and P. Vincent, “A neural probabilistic language model,” in *NIPS*, 2000.
- [6] T. Mikolov, I. Sutskever, K. Chen, G. S. Corrado, and J. Dean, “Distributed representations of words and phrases and their compositionality,” in *NIPS*, 2013.
- [7] J. Kasai, K. Qian, S. Gurajada, Y. Li, and L. Popa, “Low-resource deep entity resolution with transfer and active learning,” in *ACL*, 2019.
- [8] D. P. Kingma and M. Welling, “Auto-encoding variational bayes,” in *ICLR*, 2014.
- [9] J. Bromley, I. Guyon, Y. LeCun, E. Säckinger, and R. Shah, “Signature verification using a siamese time delay neural network,” in *NIPS*, 1993.
- [10] A. K. Elmagarmid, P. G. Ipeirotis, and V. S. Verykios, “Duplicate record detection: A survey,” *IEEE Trans. Knowl. Data Eng.*, vol. 19, no. 1, 2007.
- [11] L. Getoor and A. Machanavajjhala, “Entity resolution: Theory, practice & open challenges,” *VLDB*, vol. 5, no. 12, 2012.
- [12] R. Maskat, N. W. Paton, and S. M. Embury, “Pay-as-you-go configuration of entity resolution,” *Trans. Large Scale Data Knowl. Centered Syst.*, vol. 29, 2016.
- [13] W. Fan, X. Jia, J. Li, and S. Ma, “Reasoning about record matching rules,” *VLDB*, vol. 2, no. 1, 2009.
- [14] R. Singh, V. V. Meduri, A. K. Elmagarmid, S. Madden, P. Papotti, J. Quiané-Ruiz, A. Solar-Lezama, and N. Tang, “Generating concise entity matching rules,” in *SIGMOD*, 2017.
- [15] M. Bilenko and R. J. Mooney, “Adaptive duplicate detection using learnable string similarity measures,” in *SIGKDD*, 2003.
- [16] P. Konda, S. Das, P. S. G. C., A. Doan, A. Ardalan, J. R. Ballard, H. Li, F. Panahi, H. Zhang, J. F. Naughton, S. Prasad, G. Krishnan, R. Deep, and V. Raghavendra, “Magellan: Toward building entity matching management systems,” *VLDB*, vol. 9, no. 12, 2016.
- [17] C. Gokhale, S. Das, A. Doan, J. F. Naughton, N. Rampalli, J. W. Shavlik, and X. Zhu, “Corleone: hands-off crowdsourcing for entity matching,” in *SIGMOD*, 2014.
- [18] J. Wang, T. Kraska, M. J. Franklin, and J. Feng, “Crowder: Crowdsourcing entity resolution,” *VLDB*, vol. 5, no. 11, 2012.
- [19] R. Wu, S. Chaba, S. Sawlani, X. Chu, and S. Thirumuruganathan, “Zeroer: Entity resolution using zero labeled examples,” in *SIGMOD*, 2020.
- [20] H. Nie, X. Han, B. He, L. Sun, B. Chen, W. Zhang, S. Wu, and H. Kong, “Deep sequence-to-sequence entity matching for heterogeneous entity resolution,” in *CIKM*, 2019.
- [21] Y. Bengio, A. C. Courville, and P. Vincent, “Representation learning: A review and new perspectives,” *IEEE Trans. Pattern Anal. Mach. Intell.*, vol. 35, no. 8, 2013.
- [22] S. J. Pan and Q. Yang, “A survey on transfer learning,” *IEEE Trans. Knowl. Data Eng.*, vol. 22, no. 10, 2010.
- [23] D. J. Rezende, S. Mohamed, and D. Wierstra, “Stochastic backpropagation and approximate inference in deep generative models,” in *ICML*, ser. JMLR Workshop and Conference Proceedings, vol. 32, 2014.
- [24] M. I. Jordan, Z. Ghahramani, T. S. Jaakkola, and L. K. Saul, “An introduction to variational methods for graphical models,” *Mach. Learn.*, vol. 37, no. 2, 1999.
- [25] M. J. Beal, “Variational algorithms for approximate bayesian inference,” Ph.D. dissertation, University College London, UK, 2003.
- [26] B. Settles, “Active learning literature survey,” University of Wisconsin-Madison, Computer Sciences Technical Report 1648, 2009.
- [27] K. Qian, L. Popa, and P. Sen, “Active learning for large-scale entity resolution,” in *CIKM*, 2017.
- [28] V. V. Meduri, L. Popa, P. Sen, and M. Sarwat, “A comprehensive benchmark framework for active learning methods in entity matching,” in *SIGMOD*, 2020.
- [29] T. R. Davidson, L. Falorsi, N. D. Cao, T. Kipf, and J. M. Tomczak, “Hyperspherical variational auto-encoders,” in *Proceedings of the Thirty-Fourth Conference on Uncertainty in Artificial Intelligence, UAI 2018, Monterey, California, USA, August 6-10, 2018*, 2018.
- [30] H. Kushner and G. Yin, *Stochastic Approximation and Recursive Algorithms and Applications*, ser. Stochastic Modelling and Applied Probability, 2003.
- [31] R. Alghamdi and K. Alfaifi, “A survey of topic modeling in text mining,” *International Journal of Advanced Computer Science and Applications*, vol. 6, 01 2015.
- [32] S. Dumais, “Latent semantic analysis,” *Annual Review of Information Science and Technology*, vol. 38, 01 2004.
- [33] D. M. Blei, A. Y. Ng, and M. I. Jordan, “Latent dirichlet allocation,” *J. Mach. Learn. Res.*, vol. 3, 2003.
- [34] P. Bojanowski, E. Grave, A. Joulin, and T. Mikolov, “Enriching word vectors with subword information,” *Trans. Assoc. Comput. Linguistics*, vol. 5, 2017.
- [35] J. Pennington, R. Socher, and C. D. Manning, “Glove: Global vectors for word representation,” in *EMNLP*, 2014.
- [36] D. Tang, F. Wei, N. Yang, M. Zhou, T. Liu, and B. Qin, “Learning sentiment-specific word embedding for twitter sentiment classification,” in *ACL*, 2014.
- [37] A. Bogatu, A. A. A. Fernandes, N. W. Paton, and N. Konstantinou, “Dataset discovery in data lakes,” in *ICDE*, 2020.
- [38] S. R. Bowman, L. Vilnis, O. Vinyals, A. M. Dai, R. Józefowicz, and S. Bengio, “Generating sentences from a continuous space,” in *SIGNLL*, 2016.
- [39] P. Neculoiu, M. Versteegh, and M. Rotaru, “Learning text similarity with siamese recurrent networks,” in *Rep4NLP@ACL*, 2016.
- [40] A. Mallasto and A. Feragen, “Learning from uncertain curves: The 2-wasserstein metric for gaussian processes,” in *NIPS*, 2017.
- [41] G. Gallego, C. Cuevas, R. Mohedano, and N. García, “On the mahalanobis distance classification criterion for multidimensional normal distributions,” *IEEE Transactions on Signal Processing*, vol. 61, 09 2013.
- [42] M. Deudon, “Learning semantic similarity in a continuous space,” in *NIPS*, 2018.
- [43] A. Beygelzimer, D. J. Hsu, J. Langford, and T. Zhang, “Agnostic active learning without constraints,” in *NIPS*, 2010.
- [44] J. T. Ash, C. Zhang, A. Krishnamurthy, J. Langford, and A. Agarwal, “Deep batch active learning by diverse, uncertain gradient lower bounds,” in *ICLR*, 2020.
- [45] P. Indyk and R. Motwani, “Approximate nearest neighbors: Towards removing the curse of dimensionality,” in *STOC*, 1998.
- [46] M. Datar, N. Immorlica, P. Indyk, and V. S. Mirrokni, “Locality-sensitive hashing scheme based on p-stable distributions,” in *Symposium on Computational Geometry*, 2004.
- [47] B. W. Silverman, *Density Estimation for Statistics and Data Analysis*, 1986.
- [48] S. Hochreiter and J. Schmidhuber, “Long short-term memory,” *Neural Computation*, vol. 9, no. 8, 1997.